Canadian Chemical Transactions

ISSN 2291-6458 (Print), ISSN 2291-6466 (Online)
Year 2014 | Volume 2 | Issue 2| Page 134-148

Research Article

DOI:10.13179/canchemtrans.2014.02.02.0081

A DFT Study of the Triplet Excited States of Iridium(III) Complexes with Terpyridine Ligands

Naokazu Y.[1], Shinichi Y.[2]*, Shigeyoshi S.[2], Nobuko K.[3], Tsuyoshi I.[3], and Hiroshi T. [1]

[1]*Department of Chemistry, Faculty of Science, Nara Women's University, Kitauoya-cho, Nara 630-8506, Japan*
[2]*Fukui Institute for Fundamental Chemistry, Kyoto University, Takano-Nishihiraki-cho34-4, Sakyo-ku, Kyoto 606-8103, Japan*
[3]*Department of Applied Chemistry, Graduate School of Engineering, Osaka University, Osaka 565-0871, Japan*

[*]*Corresponding Author, E-mail*: *yamabes@fukui.kyoto-u.ac.jp*

Received: *December 31, 2013* ***Revised:*** *January 19, 2013* ***Accepted:*** *January 23, 2014* ***Published:*** *January 24, 2014*

Abstract: Density functional theory (DFT) calculations were performed to examine the triplet states of ten iridium(III) complexes and the relationship between these states and the emission spectra of the complexes. Those complexes have ligands of terpyridine derivatives. Among them, complexes [IrBr(phen)(terpy)]$(PF_6)_2$ (**2**) and [IrBr(phen)(tterpy)]$(PF_6)_2$ (**3**) were newly synthesized for this study and exhibited pronounced phosphorescent emission. Here, phen is 1,10-phenanthroline, terpy is 2,2':6',2''-terpyridine and tterpy is 4'-(4-tolyl)-2,2':6',2''-terpyridine.

All complexes were calculated to possess either one or two low-energy triplet excited states, designated as T_b and T_c. The T_c triplet states arise typically from the one-electron excitation from HOMO of the out-of-phase $5d_\pi$-π overlap to the low-lying vacant orbital of the ($5d_\sigma$-N_σ) antibonding overlap. The T_b states of the complexes are primarily associated with metal-to-ligand charge transfer (MLCT) and π-π^* transitions. The energy gaps between T_b triplet states and ground states were compared with those corresponding to peaks in the emission spectra of **2**, **3** and the other eight reported complexes. A high degree of the correlation between calculated and observed energies was obtained.

Keywords: Iridium Complexes; Terpyridine; DFT; Emission; A Double Triplet State

1. INTRODUCTION

Luminescent transition metal complexes have received increasing attention due to their potential applications as organic light-emitting diodes [1-7]. The polypyridine complexes of second-row and third-row d^6 transition metals in particular show useful spectroscopic and photophysical properties and have been widely studied. Those complexes exhibit strong phosphorescence due to the mixing of singlet and triplet excited states via spin-orbit coupling. Many computational studies have been carried out with the aim of better understanding the photophysical properties of such metal complexes [8-14].

ISSN 2291-6458 (Print), ISSN 2291-6466 (Online)
Year 2014 | Volume 2 | Issue 2| Page 134-148

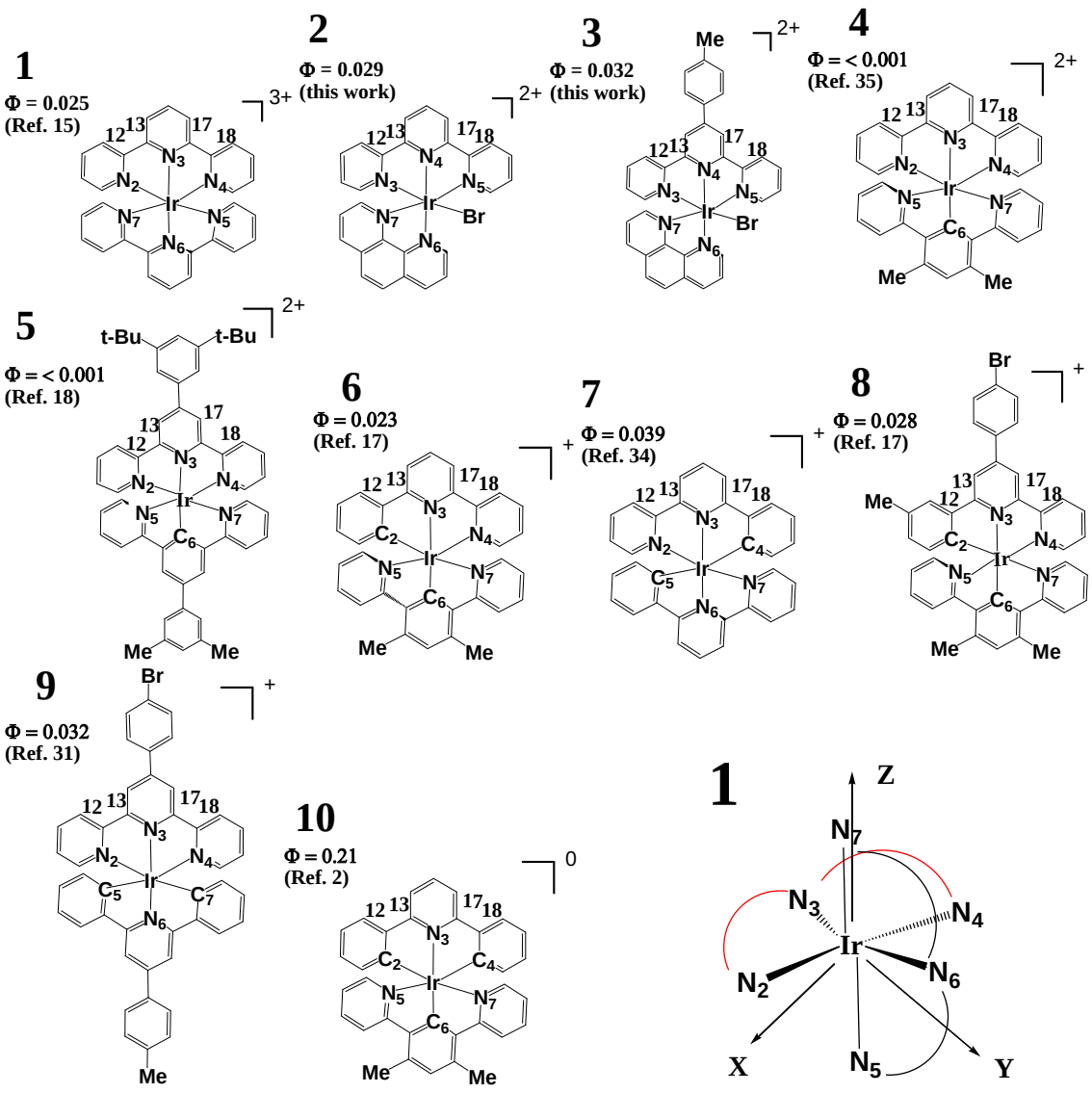

Figure 1. Structural formulae of the iridium(III) complexes calculated in this work. Nitrogen and some carbon atoms are numbered for explanations in the text. Reported quantum yields (Φ) and reference numbers are shown for complexes. In **4**-**10** complexes, some N atoms in **1** are replaced by carbanions. The central part of the complex **1** is shown in the broken box for the three-dimensional presentation of nitrogen atoms.

Complexes based on Ir(III) are generally resistant to ligand exchange. This property is actually useful in an organic light-emitting material, and accordingly many Ir(III) complexes exhibit high quantum yields in their emission spectra. Ligands containing the bond sequences C-N-C-, N-C-N-, N-N-C- or N-N-N in addition to that of C-N or N-N [15-18] are often incorporated in emissive transition metal

ISSN 2291-6458 (Print), ISSN 2291-6466 (Online)
Year 2014 | Volume 2 | Issue 2| Page 134-148

complexes. Ir(III) complexes with those ligands exhibit a variety of emission wavelengths, corresponding to colors ranging from yellow to red. Although the majority of those compounds are strongly emissive, some complexes exhibit low quantum yields. Such low quantum yields have been attributed to cleavage of the Ir-ligand bond in the triplet excited states [19-21]. In our previous work [21], phen containing iridium complexes were examined experimentally and computationally. However, the mechanism of the process, particularly in well studied terpyridine-containing Ir complexes, is not clear. In order to improve the low quantum yields of those complexes, it is therefore necessary to clarify the electronic structures, geometries and bonding associated with the triplet excited states.

In addition to the unclear mechanism of the low quantum yields, it has not been investigated by DFT calculations whether two or more triplet states are present in those complexes. The purpose of this study is to reveal the electronic structures and geometries of the triplet states of various Ir(III) complexes, and to understand the effects of these factors on the emission spectra of the complexes. DFT calculations were carried out to investigate ten Ir(III) complexes containing terpyridine derivatives as ligands. Among them, two new Ir(III) complexes **2** and **3** were synthesized and their emission spectra were also examined.

2. COMPUTATIONAL METHODS

DFT calculations for ten complexes were performed. The Gaussian09 program package [22] was used. The Becke three parameter hybrid exchange and the Lee-Yang-Parr correlation functional (B3LYP) [23,24] were applied to the calculations. Geometries in the singlet closed-shell and triplet biradical states were optimized by the R(U)B3LYP method. As the basis sets, LANL2DZ [25] was used for the Ir^{3+} ion, 6-311+G(d) was used for Br^- and 6-311G(d) [26] was used for C, H and N atoms. Partial optimizations were initially used to determine the approximate gometries of the various triplet states (as an example, T_c states were first optimized by applying a fixed long Ir-N distance). Subsequently, full optimization was performed to obtain stationary points or respective triplet states. Mulliken spin densities with the B3LYP method were computed, which has proven to provide reliable results [27] in comparison with other theoretical methods such as natural bond orbitals (NBO) or atoms in molecules (AIM).

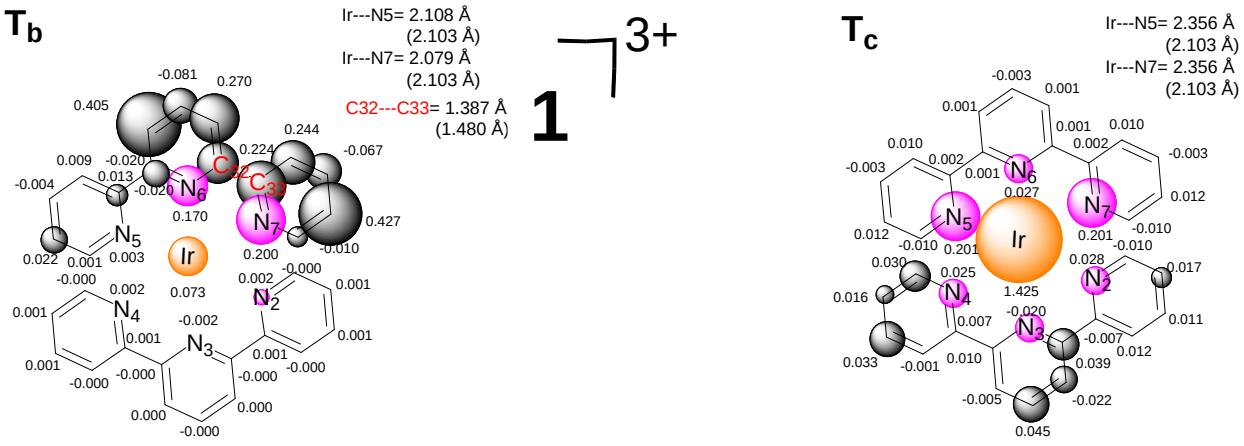

Figure 2. Distributions of Mulliken spin densities in two triplet states of the trivalent complex **1**. Magnitudes are expressed by circle size. Distances which are appreciably different from those in the ground state (S_0, in parentheses) are also shown. (See Table S2 for a summary of these data. Cartesian coordinates of the optimized geometries are also provided in Supporting Information.)

ISSN 2291-6458 (Print), ISSN 2291-6466 (Online)
Year 2014 | Volume 2 | Issue 2| Page 134-148

The energy difference between the ground and triplet states were calculated by that of the sum of the SCRF = PCM [28-30] containing electronic energy and the gas-phase zero-point vibrational one. TDDFT calculations were made to examine the electron excitation affording a specific triplet state. Also, they were carried out to compare with UV absorption spetra of two new complexes (**2** and **3**).

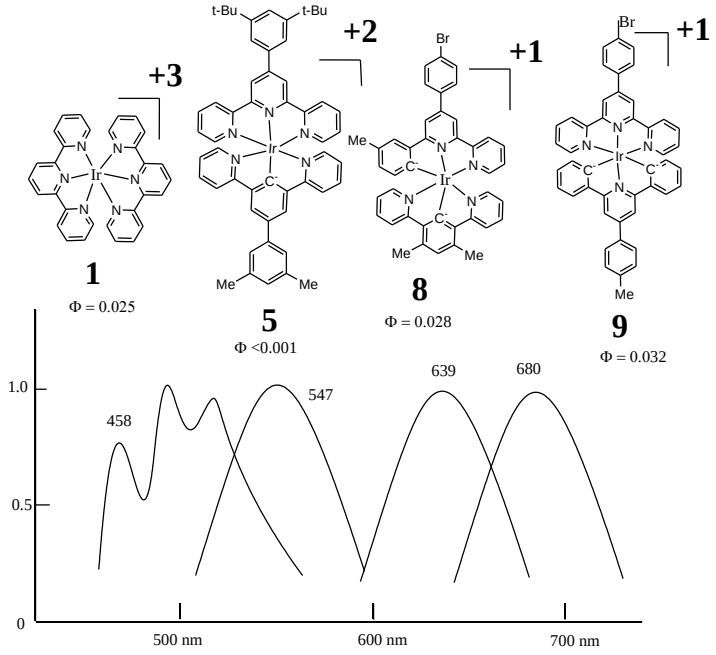

Scheme 1: Normalized emission spectra from the literature; **1** from Ref. **[**15], **5** and **8** from Refs. [18,17], respectively, and **9** from Ref. [31].

3. RESULT AND DISCUSSION

3.1 Models of complexes for DFT calculations

The structural formulae of the iridium(III) complexes examined are shown in Figure 1. For **1**, (**2**-**5**), (**6**-**9**) and **10**, the ionic valences are +3, +2, +1 and 0, respectively. In **3**, **5**, **8** and **9** aryl groups are attached to 4'- position of the terpy derivatives. Among ten complexes, **2** and **3** are new ones. Their syntheses and spectroscopic analyses are described in Expt. S1～S4 (Supporting Information). For complexes **6**-**10**, the reason why carbanion-containing ligands generally enhance the emission spectra was investigated.

The emission spectrum of the complex **1** [15] is illustrated in Scheme 1, along with the spectra of three additional carbanion-containing complexes: **5** [18], **8** [17], **9** [31]. These complexes exhibit a variety of emission wavelengths, corresponding to colors ranging from yellow to red. Complexes **1**, **8** , and **9** except **5** are strongly emissive.

3.2 Triplet states of ten complexes in Figure 1

Distributions of Mulliken spin densities in the triplet states of the trivalent complex **1** are shown in Figure 2. Magnitudes are expressed by circle size. Distances which are appreciably different from those in the ground state (S_0) are also provided. Two triplet states, defined here as

ISSN 2291-6458 (Print), ISSN 2291-6466 (Online)
Year 2014 | Volume 2 | Issue 2| Page 134-148

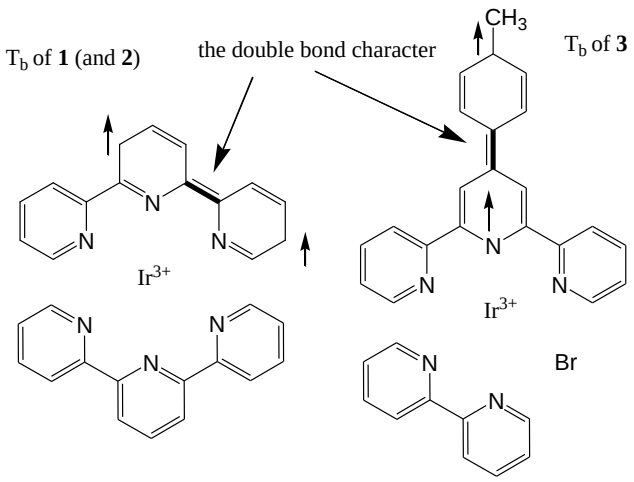

Scheme 2. Spin distributions in the triplet T_b states, in which the π-π* transition is the major component. Upward arrows stand for electron spins

T_b and T_c, were determined by DFT calculations. The T_b state is characterized by localization of the spin distribution on the connected six-membered rings of the terpy ligand, whereas the T_c state is defined by localization of the distribution on the Ir metal. In the T_b state of **1**, the C32-C33 bond length of 1.387 Å is shorter than in the ground state S_0 of **1** (1.480 Å). The shortening is explicable in terms of a resonance structure depicted in the left of Scheme 2. The Ir-N5 and Ir-N7 distances (2.108 Å and 2.079 Å) in T_b are smaller than those (2.356 Å) in T_c. The T_c state is characterized by the localization of spin distributions on the Ir^{3+} and by elongated Ir-N bonds. The distance 2.356 Å in the T_c state is larger than 2.103 Å in S_0. Consequently, almost invariance or lengthening of the Ir-N bond can typically be used as an indicator of the nature of the triplet state (i.e. whether the state is T_b or T_c).

Figure 3 presents distributions of Mulliken spin densities in the triplet states of the divalent complexes **2**, **3, 4** and **5**. In the T_b state of **2**, the C17-C18 bond length of 1.402 Å is shorter than in the ground state S_0 of **2** (1.478 Å) (see also Table S2 in Supporting Information). Interestingly, there are differences between **2** and **3** in the localization of spin densities. These differences may be understood by considering the parallel spins illustrated in Scheme 2.

In **2**, the spin density value of Ir (0.306) of the T_b state is low. This low value suggests that the state consists of small metal-to-ligand charge transfer (MLCT) and large π-π* transition components.

In **1**, the T_b state is due almost entirely to π-π* transitions as a result of the low-lying (inactive) $5d_\pi$ lone-pair orbitals of Ir^{3+} and their correspondingly small contribution to the triplet state. In contrast, in **2** and **3**, the out-of-phase combination of the bromide 4pπ and Ir $5d_\pi$ lone-pair orbitals results in a high-lying occupied orbital. This orbital readily allows the MLCT transition (see Scheme 3). Therefore, in **2** and **3**, T_b's are composed of a relatively equal mixture of MLCT and π-π* transitions. As a result of the MLCT transition, the Ir-N7 distance of **2** in the T_b state (2.051 Å) is slightly smaller than that in the S_0 state (2.089 Å). The electron loss in the out-of-plase orbital associated with the MLCT transition strengthens the Ir-Br bond of **2**. Consequently, the bond length in the T_b state is smaller than in the S_0 state (2.487 Å compared to 2.524 Å).

ISSN 2291-6458 (Print), ISSN 2291-6466 (Online)
Year 2014 | Volume 2 | Issue 2| Page 134-148

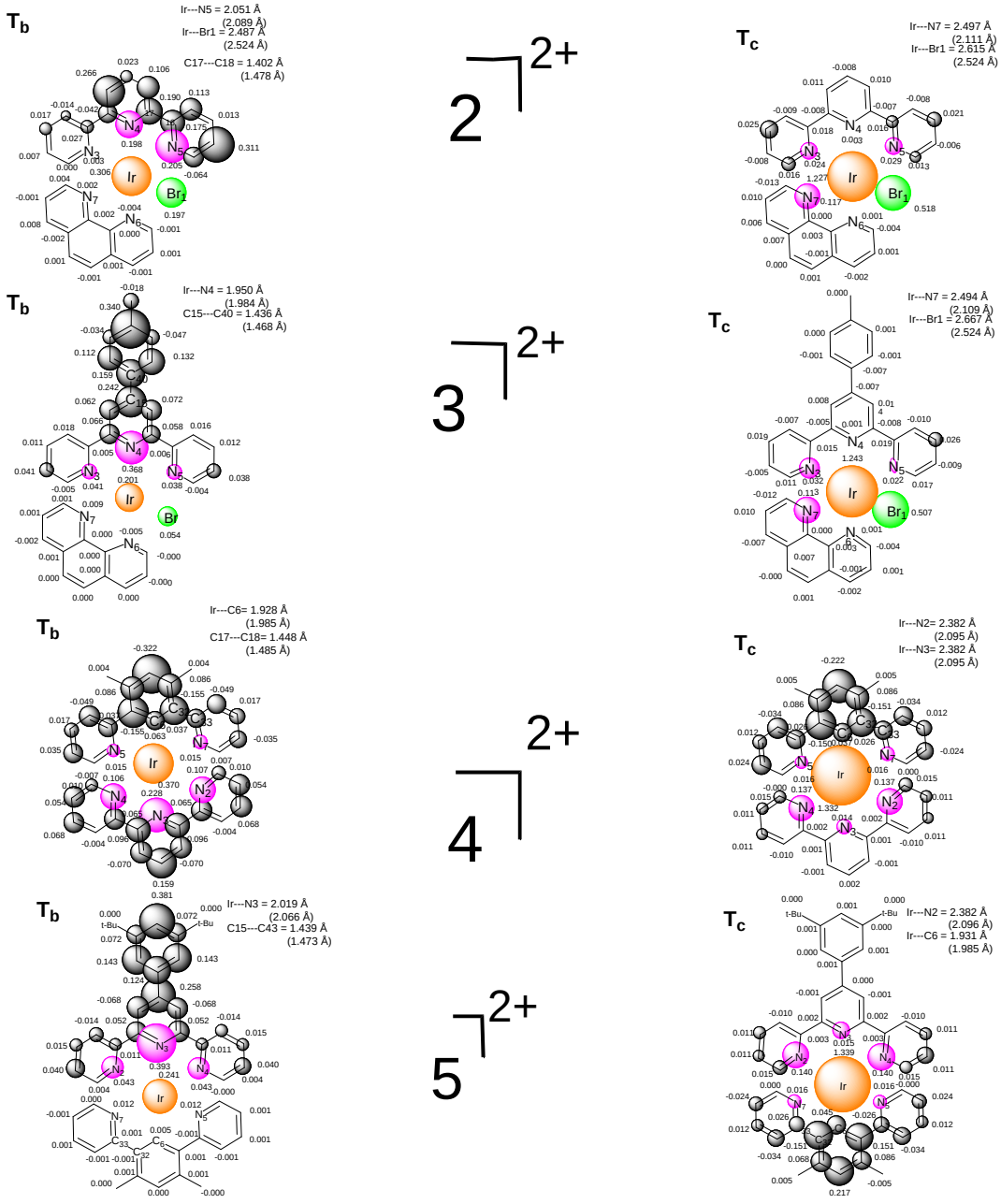

Figure 3. Distributions of Mulliken spin densities in the triplet states of the divalent complexes **2**, **3, 4** and **5**

Figure 3 also shows the triplet states obtained for the complexes **4**, and **5**. These were found also to have both T_b and T_c states. In T_c of **4** and **5** , the large spin density values 1.332 and 1.339 of Ir were obtained, respectively. These large values indicate that the T_c states consist of "d-d* transition" components ,which will be explained in Scheme 5.

Figure 4 shows distributions of spin densities of the monovalent complexes **6**, **7, 8** and **9**. In **6**, **8** and **9**, both T_b and T_c states were found, while the complex **7** does not have the T_c state.

ISSN 2291-6458 (Print), ISSN 2291-6466 (Online)
Year 2014 | Volume 2 | Issue 2| Page 134-148

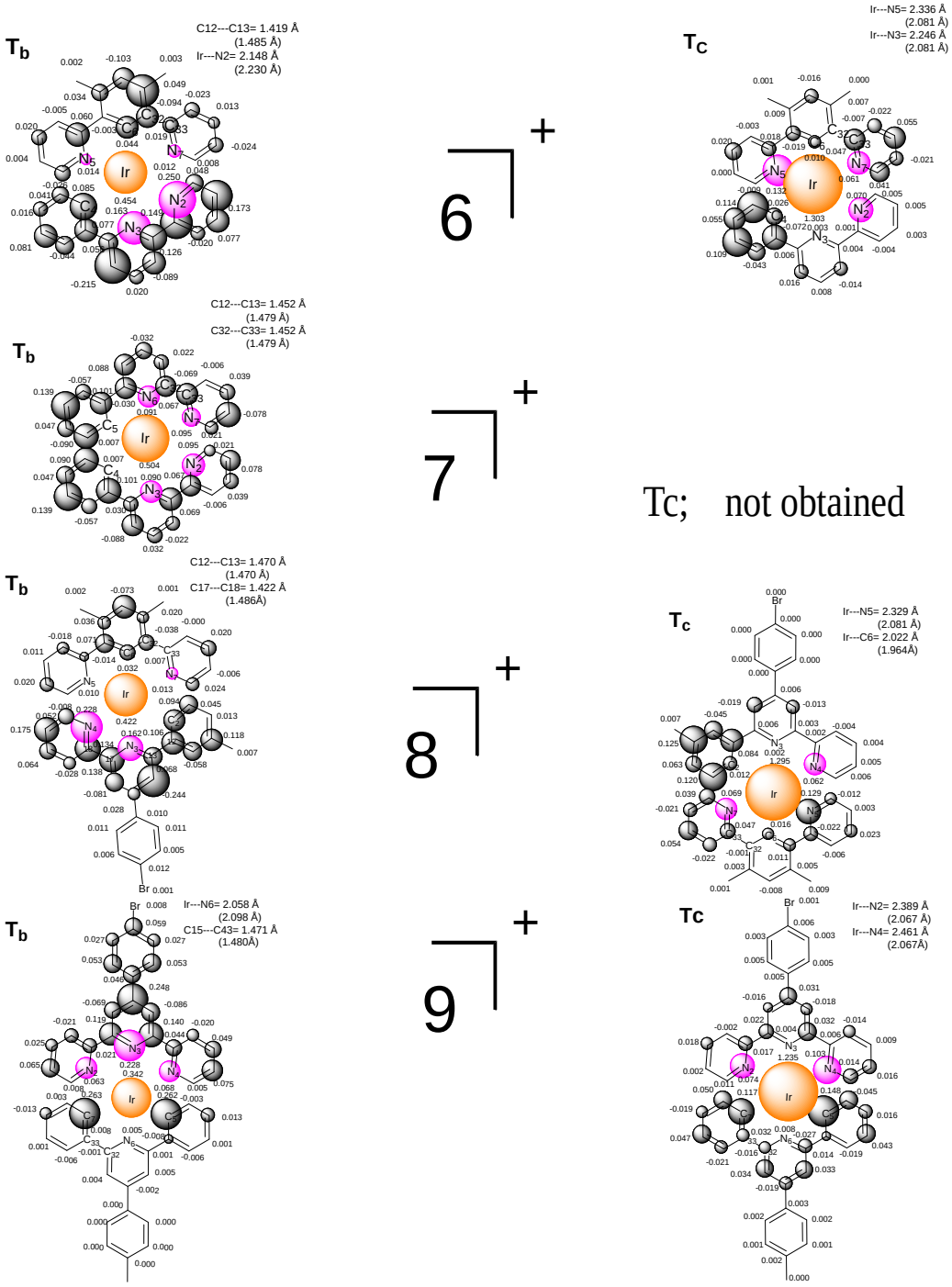

Figure 4. Distributions of Mulliken spin densities in the triplet states of the monovalent complexes **6**, **7, 8** and **9**.

ISSN 2291-6458 (Print), ISSN 2291-6466 (Online)
Year 2014 | Volume 2 | Issue 2| Page 134-148

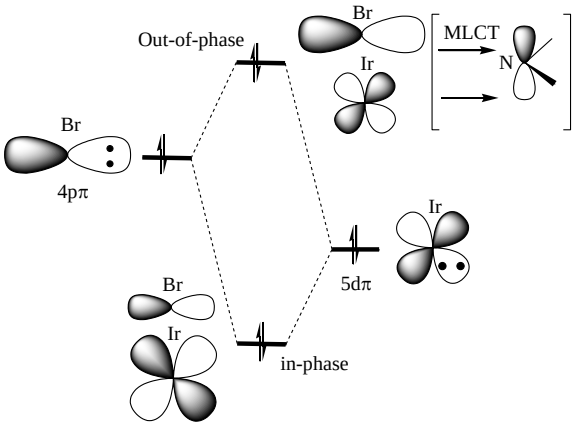

Scheme 3. In-phase and out-of-phase overlaps of Ir $5d_{\pi}$ and Br $4p_{\pi}$ orbitals. MLCT results from electron excitation from the high-lying out-of-phase orbital.

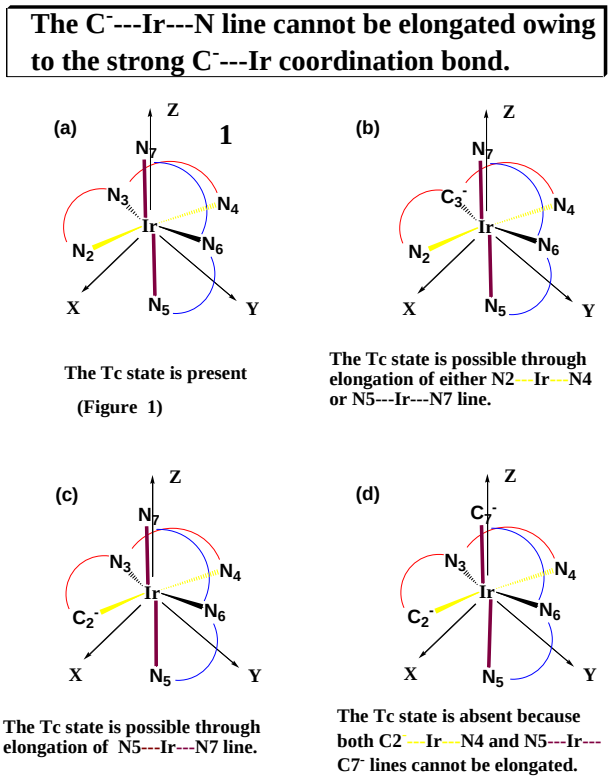

Scheme 4. The effects of carbon anions on coordination bonds with the Ir^{3+} center. (a) The basic complex **1**. (b), (c) and (d) Three substitutions of C^- by N. Bonds in the series N3-Ir-N6 and $C3^-$-Ir-N6 are strong and are not associated with the formation of the T_c state.

ISSN 2291-6458 (Print), ISSN 2291-6466 (Online)
Year 2014 | Volume 2 | Issue 2| Page 134-148

Figure 5 shows distributions of Mulliken spin densities in the triplet states of the zerovalent (neutral) complex **10**. Complex **10** was found to have both T_b and T_c states. In the seven complexes **4**-**10** shown in Figures 3, 4, 5, the spin densities on the Ir^{3+} of T_b states were found to be relatively insensitive to variations in ionic valence, which is in contrast to the different densities of three complexes **1**-**3** in Figures 2, 3.

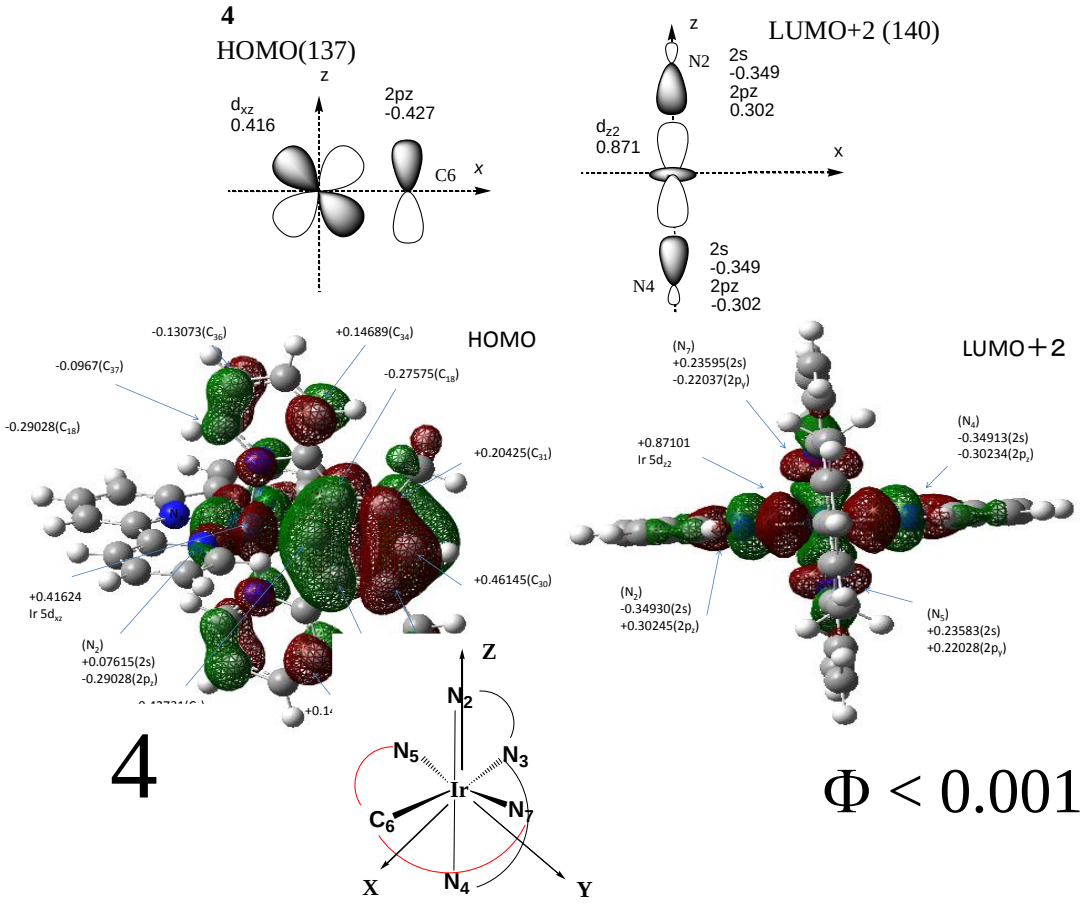

Scheme 5. Orbital shapes and coefficients of HOMO and LUMO+2 in the complex **4**

3.3 Discussions of T_c states

First, the factors which affect the presence or absence (in the complex **7**) of the T_c state are explained in Scheme 4. Specifically, the model (d) in Scheme 4 shows the case where the T_c state is absent by the prohibited enlargement of the C2$^-$-Ir-N4 and C7$^-$-Ir-N5 distances (hence the designation of T_c as "not obtained" in **7** of Figure 4). All complexes except **7** have N-Ir-N bonds capable of elongation and therefore have T_c states.

Second, the character of the T_c state is scrutinized. The T_c states are associated with high spin densities (on the order of 1.2 to 1.3) at the Ir^{3+} center. Through the heavy-atom effect, these contribute to significant spin-orbit interaction and hence to non-radiative relaxation. Therefore, when the T_c state is stable [32], non-radiative relaxation is enhanced and the quantum yield of the emission inevitably decreases. It is known that the non-radiative decay rate of an excited state increases exponentially as the

ISSN 2291-6458 (Print), ISSN 2291-6466 (Online)
Year 2014 | Volume 2 | Issue 2| Page 134-148

energy gap between the triplet and ground states becomes small [33]. In this respect, the remarkably large difference of quantum yields $\Phi < 0.001$ of **4** and $\Phi = 0.21$ of **10** would come from that of their T_c energy levels. **4** and **10** are isoelectronic complexes. It is examined how their T_c states are generated by the electron excitation in the ground state (S_0). In the complex **4**, the HOMO → LUMO+2 excitation which is included in the 6-th excited state (by TDDFT) gives the following ($S_0 \rightarrow T_c$) geometrical change (Scheme 5).

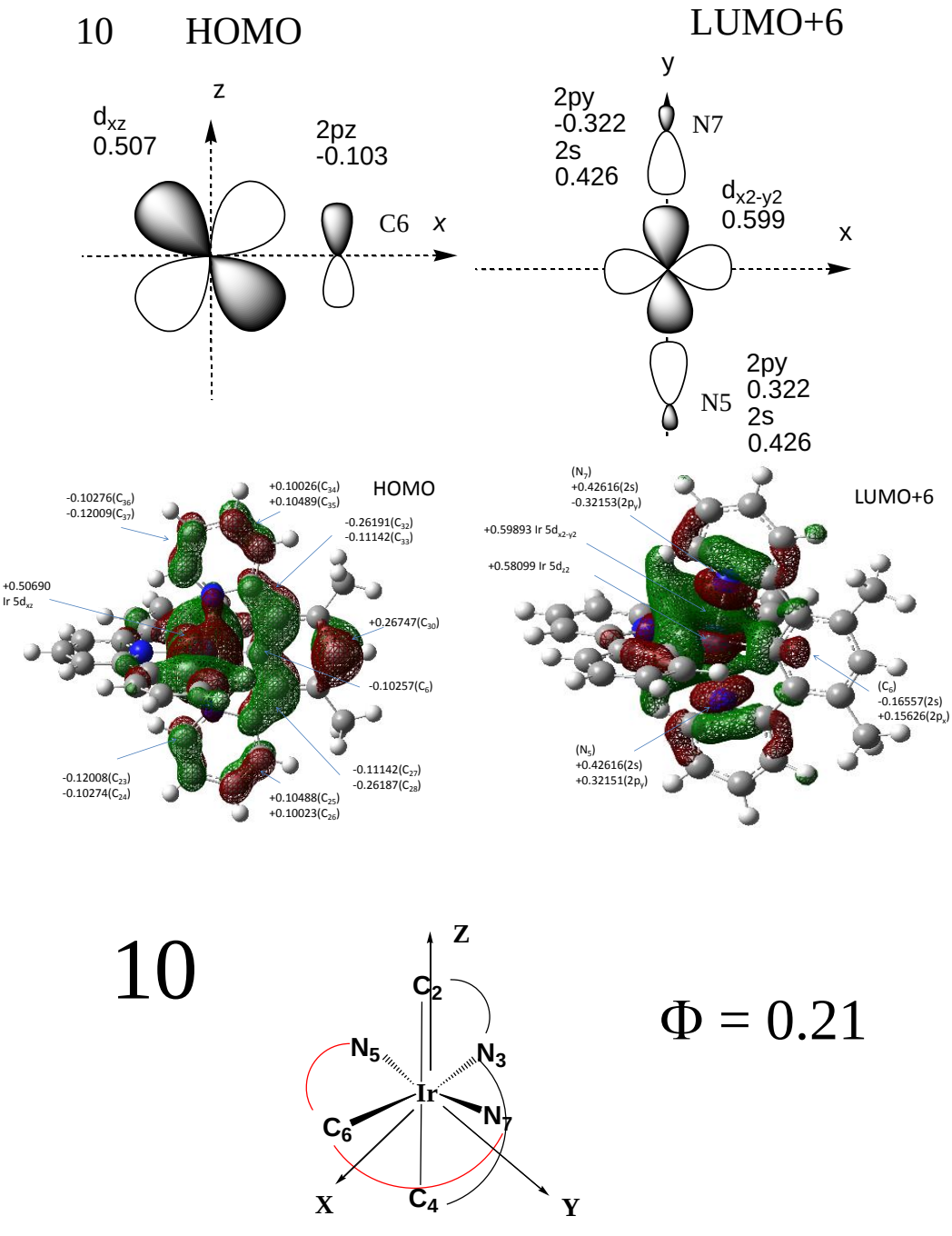

Scheme 6: Orbital shapes and coefficients of HOMO and LUMO+6 in the complex **10**

ISSN 2291-6458 (Print), ISSN 2291-6466 (Online)
Year 2014 | Volume 2 | Issue 2| Page 134-148

By the one electron loss of HOMO, the [$5d_{xz}$ - $2p_z(C_6)$] antibonding character is weakened, which results in the shortening of the Ir- C_6 distance, 1.985 Å in S_0 → 1.929 Å in T_c (as shown in Figure 3). On the other hand, by the electron acceptance in LUMO+2, the antibonding character in Ir-N_2 and Ir-N_4 becomes elicited. Accordingly, these distances are enlarged, 2.095 Å in S_0 → 2.382 Å in T_c. The similar (π-σ^*) type one-electron excitation is (HOMO → LUMO+6) in **10**, which is shown in Scheme 6. The large excitation energy is required, which will give the unstable T_c state. Thus, the contrast of $\Phi < 0.001$ of **4** [35] vs. $\Phi = 0.21$ of **10** [2] is thought to arise from energy levels (low in **4** vs. high in **10**) of T_c states.

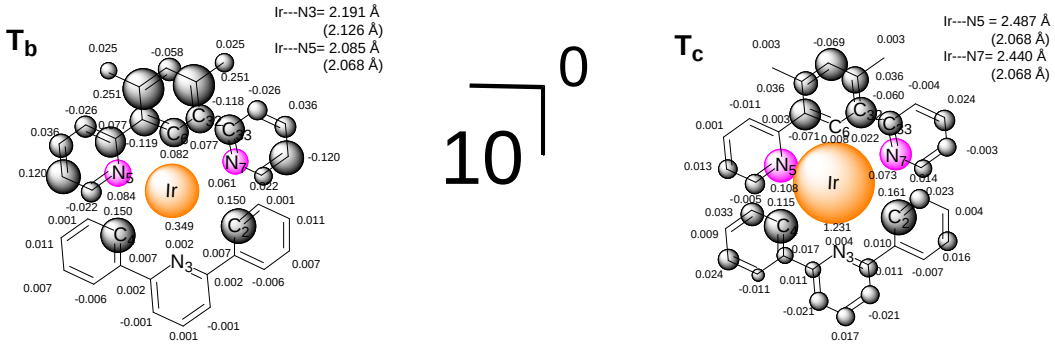

Figure 5. Distributions of Mulliken spin densities in the triplet states of the zerovalent complex **10**

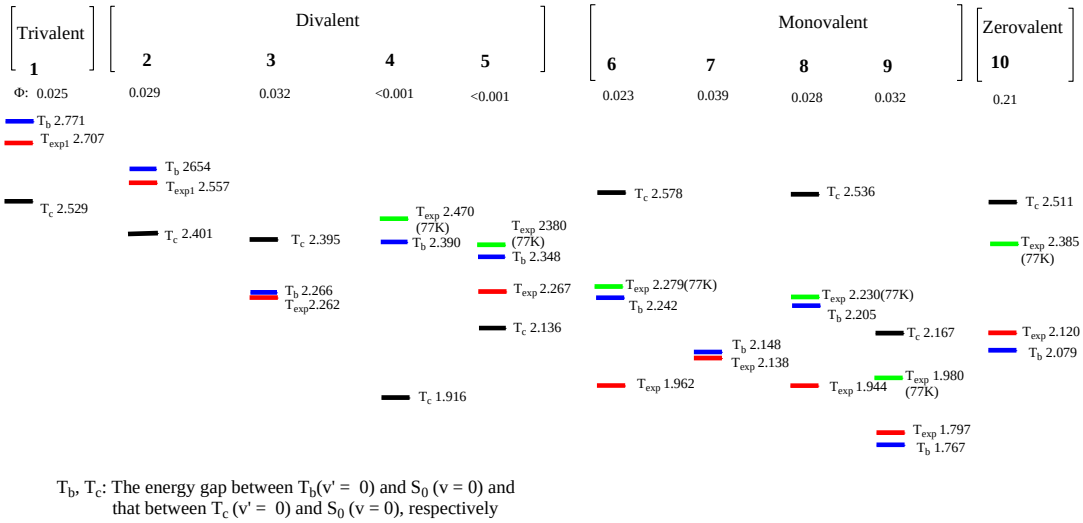

Figure 6. Energy diagrams of the triplet states of iridium complexes. Calculated energies (eV) are for triplet states shown in Figures 2, 3, 4 and 5 relative to those of the corresponding ground states. Energies shown in red are experimental data (**1** from Ref. [15], **4** from Ref. [35], **5** from Ref. [18], **6** from Ref. [17], **7** from Ref. [34], **10** from Ref. [2], **8** from Ref. [17], **9** from Ref. [31] and **2** and **3** from this work)

ISSN 2291-6458 (Print), ISSN 2291-6466 (Online)
Year 2014 | Volume 2 | Issue 2| Page 134-148

3.4 Energies of the calculated triplet states

Figure 6 summarizes the differences of the sum of electronic and zero-point vibrational energies between the calculated triplet states (T_b and T_c) and ground states (S_0's). The experimental energy levels (T_{exp}) in this figure are taken from peaks observed in the emission spectra found in references [2, 15, 17, 18, 31, 34, 35] as well as from spectra obtained in Table S1 of the present work for **2** and **3**. The data in this figure demonstrate that the calculated (T_b - S_0) energy differences are closer to the experimentally derived values than are the (T_c - S_0) differences. For example, in the case of **8**, the calculated value for T_b of 2.205 eV is almost identical to the experimental value of 2.230 eV (77K), while the value for T_c is 2.536 eV. The T_b state is thought to be the emitter triplet state, while the T_c state is considered to be associated with non-radiative decay.

In the case of the divalent complexes **4** and **5**, the T_c energy levels are low (1.916 eV and 2.136 eV), which would come to the low quantum yields $\Phi \leq 0.001$. The contrast between (HOMO → LUMO+2) in **4** and (HOMO → LUMO+6) in **10** is correctly reflected in the significantly different T_c energies, 1.916 eV of **4** and 2.511 eV of **10**, where the more stable T_c state corresponds to the enhanced non-radiative decay.

4. CONCLUSION

In this work, DFT calculations of ten iridium(III) complexes were carried out to analyze their triplet states. These electronic structures of a variety of ionic valences were investigated. Almost all of the complexes were found to have two triplet states, T_b and T_c. The T_b state represents a combination of π-π* and MLCT transitions, and the relative proportions of these two components vary with the ionic valence. The calculated (T_b - S_0) energy differences were found to be in good agreement with energy values derived experimentally from measured emission wavelengths.

The T_c state is brought about by the elongation of the collinear N-Ir-N coordination bond. This state is associated with the transition depicted in Scheme 5 and 6 and localization of spin density at the Ir center. The transition is the embodiment of the so called (d, d^*) transition. Therefore, when the energy level of the T_c state is low, non-radiative relaxation becomes dominant and accordingly the emission quantum yield is poor.

This study seems to be successful in elucidating the specific characteristics of the two triplet states and is able to determine that the T_b state is the source of the phosphorescent emission of those complexes.

ACKNOWLEDGEMENT

This work is financially supported by the Grants-in-Aid from the Ministry of Education, Culture, Science, Sport, and Technology by Grants-in-Aid of Specially Promoted Science and Technology (No. 22000009) and the Grand Challenge Project (IMS, Okazaki, Japan). We are also thankful to the computational facility at the Institute of Molecular Science, Okazaki, Japan.

SUPPORTING INFORMATION

Table S1 for absorption and emission properties of 2 and 3. Figure S1a and Figure S1b for their absorption and emission spectra. Figure S2 for two vacant orbitals of the complex 4. Expt. S1～S4 for experimental methods and results. Tables S2-S7 containing geometric data and relative energies of the calculated ten complexes and the Cartesian coordinates of optimized geometries.

ISSN 2291-6458 (Print), ISSN 2291-6466 (Online)
Year 2014 | Volume 2 | Issue 2| Page 134-148

REFERENCES AND NOTES

[1] Baranoff, E.; Collin, J. –P.; Sauvage, J. –P.; Flamigni, L. From ruthenium(II) to iridium(III): 15 years of triads based on bis-terpyridine complexes. *Chem. Soc. Rev*. **2004**, *33*, 147-155.

[2] Wilkinson, A. J.; Goeta, A. E.; Foster, C. E.; Williams, J. A. G. Synthesis and Luminescence of a Charge-Neutral, Cyclometalated Iridium(III) Complex Containing N^C^N- and C^N^C-Coordinating Terdentate Ligands. *Inorg. Chem.* **2004**, *43*, 6513-6515.

[3] Dedeian, K.; Shi, J.; Shepherd, N.; Forsythe, E.; Morton, D. C. Photophysical and Electrochemical Properties of Heteroleptic Tris- Cyclometalated Iridium(III) Complexes. *Inorg. Chem.* **2005**, *44*, 4445-4447.

[4] Flamigni, L.; Venture, B.; Barigelleti, F.; Baranoff, E.; Collin, J. –P.; Sauvage, J. –P. Luminescent Iridium(III)-Terpyridine Complexes – Interplay of Ligand Centred and Charge Transfer States. *Eur. J. Inorg. Chem*. **2005**, 1312-1318.

[5] Poison, M.; Ravaglia, M.; Fracasso, S.; Garavelli, M.; Scandola, F. Iridium Cyclometalated Complexes with Axial Symmetry: Time-Dependent Density Functional Theory Investigation of trans-Bis-Cyclometalated Complexes Containing the Tridentate Ligand 2,6-Diphenylpyridine. *Inorg. Chem*. **2005**, *44*, 1282-1289.

[6] Baldo, M. A.; Lamaneky, S. Very high-efficiency green organic light-emitting devices based on electrophosphorescence. *Appl. Phys. Lett*. **1999**, *4*. 75-77.

[7] Yoshikawa, N.; Sakamoto, J.; Matsumura-Inoue, T. ; Takashima, H.; Tsukahara, K.; Kanehisa, N.; Kai, Y. Electrochemical and Phosphorescent Properties of New Ir(III) Complexes. Coordinated by Various Bipyridine Derivatives. *Anal. Sci.* **2004**, 711-716.

[8] F.-Q. Bai, J. Wang, B.-H. Xia, Q.-J. Pan, H.-X. Zhang, DFT and TD-DFT study on the electronic structures and phosphorescent properties of 6-phenyl-2,2′-bipyridine tridentate iridium(III) complexes and their isomer. *Dalton Trans.* **2012**, *41*, 8441–8446.

[9] Terki, R.; Simoneau, L.P.; Rochefort, A. Tailoring the Photoluminescence Properties of Ionic Iridium Complexes. *J. Phys. Chem. A* **2009**, *113*, 534-541.

[10] Minaev, B.; Minaeva, V.; Ågren, H. Theoretical Study of the Cyclometalated Iridium(III) Complexes Used as Chromophores for Organic Light-Emitting Diodes. *J. Phys. Chem. A* **2009,** *113*, 726-735.

[11] Coughlin, F. J.; Westrol, M. S.; Oyler, K. D.; Byrne, N.; C. Kraml,; Colman, E. Z.; Lowry, M. S.; Bernhard, S. Synthesis, Separation, and Circularly Polarized Luminescence Studies of Enantiomers of Iridium(III) Luminophores. *Inorg. Chem.* **2008**, *47*, 2039-2048.

[12] Stagni, S.; Colella, S.; Palazzi, A.; Valenti, G.; Zacchini, S.; Paolucci, F.; Marcaccio, M.; Albuquerque, R. Q.; Cola, L. De Essential Role of the Ancillary Ligand in the Color Tuning of Iridium Tetrazolate Complexes. *Inorg. Chem.* **2008**, *47*, 10509-10521.

[13] Bandini, M.; Bianchi, M.; Valenti, G.; Piccinelli, F.; Paolucci, F.; Monari, M.; Ronchi, A. U.; Marcaccio, M. Electrochemiluminescent Functionalizable Cyclometalated Thiophene-Based Iridium(III) Complexes. *Inorg. Chem*. **2010**, *49*, 1439-1448.

[14] Gu, X.; Fei, T.; Zhang, H.; Xu, H.; Yang, B.; Ma, Y.; Liu, X. Theoretical Studies of Blue-Emitting Iridium Complexes with Different Ancillary Ligands. *J. Phys. Chem. A*, **2008**, *112*, 8387-8393.

[15] Collin, J.-P.; Dixon, I. M.; Sauvage, J.P.; Williams, J. A. G.; Barigelletti, F.; Flamigni, L. Synthesis and Photophysical Properties of Iridium(III) Bisterpyridine and Its Homologues: a Family of Complexes with a Long-Lived Excited State. *J. Am. Chem. Soc.* **1999**, *121*, 5009-5016.

[16] Chen, J.-L.; Wu, Y.-H.; He, L.-H.; Wen, H.-R.; Liao, J.; Hong, R. Iridium(III) Bis-tridentate Complexes with 6-(5-Trifluoromethylpyrazol-3-yl)- 2,2′-bipyridine Chelating Ligands: Synthesis, Characterization, and Photophysical Properties. *Organometallics* **2010**, *29*, 2882-2891.

[17] Whittle, V. L.; Williams, J. A. G. A New Class of Iridium Complexes Suitable for Stepwise Incorporation into Linear Assemblies: Synthesis, Electrochemistry, and Luminescence. *Inorg. Chem*. **2008**, *47*, 6596-6607.

ISSN 2291-6458 (Print), ISSN 2291-6466 (Online)
Year 2014 | Volume 2 | Issue 2| Page 134-148

[18] Auffrant, A.; Barbieri, A.; Barigelletti, F.; Collin, J.-P.; Flamigni, L.; Sabatini, C.; Sauvage, J.-P. Dinuclear Iridium(III) Complexes Consisting of Back-to-Back tpy-(ph)n-tpy Bridging Ligands (n = 0, 1, or 2) and Terminal Cyclometallating Tridentate N-C-N Ligands. *Inorg. Chem*. **2006**, *45*, 10990-10997.

[19] Yang, L.; Okuda, F.; Kobayashi, K.; Nozaki, K.; Tanabe, Y.; Ishii, Y.; Haga, M. Syntheses and Phosphorescent Properties of Blue Emissive Iridium Complexes with Tridentate Pyrazolyl Ligands. *Inorg. Chem.***2008**, *47*, 7154-7165.

[20] Sajoto, T.; Djurovich, P. I.; Tamayo, A. B.; Oxgaard, J.; Goddard III, W. A.; Thompson, M. E. Temperature Dependence of Blue Phosphorescent Cyclometalated Ir(III) Complexes. *J. Am. Chem. Soc*. **2009**, *131*, 9813-9822.

[21] Yoshikawa, N.; Yamabe, S.; Kanehisa, N.; Inoue, T.; Takashima, H.; Tsukahara, K. Differences of Structures and Electronic Properties in the Triplet States between Dibromo and Dichloro Mononuclear Polypyridine Iridium(III) Complexes. *Bull. Chem. Soc. Jpn*. **2011**, *84*, 1347-1354.

[22] Gaussian 09, Revision B.01, Frisch, M. J.; Trucks, G. W.; Schlegel, H. B.; Scuseria, G. E.; Robb, M. A.; Cheeseman, J. R.; Scalmani, G.; Barone, V.; Mennucci, B.; Petersson, G. A.; Nakatsuji, H.; Caricato, M.; Li, X.; Hratchian, H. P.; Izmaylov, A. F.; Bloino, J.; Zheng, G.; Sonnenberg, J. L.; Hada, M.; Ehara, M.; Toyota, K.; Fukuda, R.; Hasegawa, J.; Ishida, M.; Nakajima, T.; Honda, Y.; Kitao, O.; Nakai, H.; Vreven, T.; Montgomery, J. A., Jr.; Peralta, J. E.; Ogliaro, F.; Bearpark, M.; Heyd, J. J.; Brothers, E.; Kudin, K. N.; Staroverov, V. N.; Kobayashi, R.; Normand, J.; Raghavachari, K.; Rendell, A.; Burant, J. C.; Iyengar, S. S.; Tomasi, J.; Cossi, M.; Rega, N.; Millam, N. J.; Klene, M.; Knox, J. E.; Cross, J. B.; Bakken, V.; Adamo, C.; Jaramillo, J.; Gomperts, R.; Stratmann, R. E.; Yazyev, O.; Austin, A. J.; Cammi, R.; Pomelli, C.; Ochterski, J. W.; Martin, R. L.; Morokuma, K.; Zakrzewski, V. G.; Voth, G. A.; Salvador, P.; Dannenberg, J. J.; Dapprich, S.; Daniels, A. D.; Farkas, Ö.; Foresman, J. B.; Ortiz, J. V.; Cioslowski, J.; Fox, D. J. Gaussian, Inc., Wallingford CT, 2009.

[23] Lee, C.; Yang, W.; Parr, R. G. Development of the Colle-Salvetti conelation energy formula into a functional of the electron density. *Phys. Rev*. **1988**, *B37*, 785-787.

[24] Becke, A. D. Density-functional thermochemistry. III. The role of exact exchange. *J. Chem. Phys.***1993**, *98*, 5648-5652.

[25] Hay, J.; Wadt, W. R. *Ab initio* effective core potentials for molecular calculations. Potentials for K to Au including the outermost core orbitals. *J. Chem. Phys.* **1985**, *82*, 299-310.

[26] Francl, M. M.; Petro, W. J.; Hehre, W. J.; Binkley, J. S.; Gordon, M. S.; Defrees, D. J.; Pople, J. A. Self-Consistent Molecular Orbital Methods. 23. A Polarization Basis Set for Second Row Elements. *J. Chem. Phys*. **1982**, *77*, 3654-3665.

[27] Ruiz, E.; Cirera, J.; Alvarez, S. Spin density distribution in transition metal complexes. *Coord. Chem. Rev*. **2005**, *249*, 2649-2660

[28] Cances, E.; Mennucci, B.; Tomasi, J. A New Integral Equation Formalism for the Polarizable Continuum Model: Theoretical Background and Applications to Isotropic and Anisotropic Dielectrics. *J. Chem. Phys*. **1997**, *107*, 3032-3041.

[29] Cossi, M.; Barone, V.; Mennucci, B.; Tomasi, Ab initio study of ionic solutions by a polarizable continuum dielectric model. *J. Chem. Phys. Lett*. **1998**, *286* , 253-260.

[30] Mennucci, B.; Tomasi, J. Continuum solvation models: A new approach to the problem of solute's charge distribution and cavity boundaries. *J. Chem. Phys.***1997**, *106* ,5151-5158.

[31] Polson, M.; Fracasso, S.; Bertolasi, V.; Ravaglia, M.; Scandola, F. Iridium Cyclometalated Complexes with Axial Symmetry. Synthesis and Photophysical Properties of a *trans*-Biscyclometalated Complex Containing the Terdentate Ligand 2,6-Diphenylpyridine. *Inorg. Chem*. **2004**, *43*, 1950-1956.

[32] Howerton, B. S.; Heidar, D. K.; Glazer, E. C. Strained ruthenium complexes are potent light-activated anticancer agents. *J. Am. Chem. Soc*. **2012**, *134*, 8324-8327.

[33] Kasha, M. Characterization of electronic transitions in complex molecules. *Discussions of the Faraday Society*, **1950**, *9*, 14-19.

ISSN 2291-6458 (Print), ISSN 2291-6466 (Online)
Year 2014 | Volume 2 | Issue 2| Page 134-148

[34] Tinker, L. L.; Bernhard, S. Photon-Driven Catalytic Proton Reduction with a Robust Homoleptic Iridium(III) 6-Phenyl-2,2′-bipyridine Complex ([Ir(C^N^N)2]$^{+}$). *Inorg. Chem.* **2009**, *48*, 10507-10511.
[35] Wilkinson, A. J.; Puschmann, H.; Howard, J. A. K.; Foster, C. E.; Williams, J. A. G. Luminescent Complexes of Iridium(III) Containing N^C^N-Coordinating Terdentate Ligands. *Inorg. Chem.* **2006** *45* 8685-8699.

The authors declare no conflict of interest

© 2014 By the Authors; Licensee Borderless Science Publishing, Canada. This is an open access article distributed under the terms and conditions of the Creative Commons Attribution license http://creativecommons.org/licenses/by/3.0/